EEET ECOLOGICAL ENGINEERING & ENVIRONMENTAL TECHNOLOGY

Ecological Engineering & Environmental Technology 2024, 25(4), 125–142
https://doi.org/10.12912/27197050/178530
ISSN 2719-7050, License CC-BY 4.0

Received: 2023.12.16
Accepted: 2024.01.10
Published: 2024.02.25

Monthly and Annual Precipitation in Arid Environment of the Daoura Watershed (South-Eastern Morocco) – Homogenization and Trend Analysis

Yassine Chanyour[1*], Ouafaa El Achari[2], Mohamed Hanchane[2], Khalid Obda[1], Ridouane Kessabi[2]

[1] Department of Geography, Sidi Mohamed Ben Abdellah University, P.B. 59, Immouzer Road, 30000 Fez, Morocco

[2] Department of Geography, Laboratory of Territory, Heritage and History, Sidi Mohamed Ben Abdellah University, 30500 Fez, Morocco

* Corresponding author's e-mail: yassinechanyour@gmail.com

ABSTRACT

The high variability of the sub-desert climate, especially in the south-eastern region of Morocco, has severe socio-economic impacts on the inhabitant's way of life, as is the case in the Daoura watershed, where this variability is associated with droughts or exceptional rainfall. The data collected from the Guir-Ziz-Rheriss hydraulic agency were processed, corrected and analyzed using the Climatol package (version 4.0.0) developed in R software to homogenize rainfall data. Through this work, the significance and amplitudes of annual and monthly rainfall trends were defined using the Mann-Kendall test and Sens's slope estimator, while comparing the results of raw and homogenized data. The Daoura watershed has a sub-desert climate, and the homogenization process revealed a few rainfall stations with significant positive trends at confidence levels ranging from 90% to 95%. According to the raw and homogenized data, the majority of these stations are located in the High Atlas (CR1) and Anti-Atlasic (CR2) zones, where there is considerable spatiotemporal variability in rainfall from one year to the next. The essential objective of this scientific paper was to analyze the spatiotemporal variability of monthly and annual precipitation and to study their trends through rainfall data homogenized by the climatol package (version 4.0.0) from 13 stations over a period (1957–2018). The contribution of this study to science is the rainfall data it offers, which is useful for managing natural resources in sub-desert areas.

Keywords: precipitation, homogenization, Sen's Slope, trend, Daoura.

INTRODUCTION

Numerous studies have shown significant fluctuations in precipitation on both a regional and temporal scale in the Mediterranean region (Rodriguez-Puebla et al., 1998; Servat et al., 1999; Meddi et al., 2010; Taibi et al., 2013; De Luis et al., 2000). The region is distinguished by a pattern of alternating rainy and dry spells, in addition to variations in height and continentality. The influence of the Mediterranean Sea means that the region's Mediterranean-type climate extends much further into the continental mass than elsewhere and is not limited to a narrow band facing the ocean (Hoerling et al., 2012; Xoplaki et al., 2004; Bandhauer et al., 2022). The Maghreb nations of Algeria, Tunisia, and Morocco are the most severely impacted by this issue (Zamrane et al., 2021). Morocco's latitudinal position places it in a climate area where the north experiences a temperate temperature, while the south experiences a subtropical climate. Morocco's climate is classified as Mediterranean to the north and northwest, dry steppe to the northeast, as well as desert to the south and southeast by the Köppen classification. A dry season that lasts longer as it progresses from the country's west to east and north to south is a defining feature of its Mediterranean climate. The arid climates of the nation are typified by infrequent rainfall and a

significant need for water vapor. Merely 15% of the nation's land area receives half of all rainfall (Ezzine et al., 2014). There is a substantial amount of fluctuation in the space-time distribution of the average yearly precipitation. Rainfall on mountain summits can approach 1000 mm in the north, while it does not surpass 50 mm in the south (Salhi et al., 2019). Moroccan climates are also characterized by high inter-year variability in precipitation and significant temporal irregularities in precipitation, which cause periods of drought that may be followed by extremely humid intervals or intense rainfall events. (Emberger, 1971) established a regional distribution of Moroccan precipitation, and since the 1940s, researchers have examined the time-space variability of precipitation there. Since the 1980s, some people have seen a decline in rainfall; others have noted a deficit phase up to 1956, a normal phase leading to a surplus until 1970, and a protracted drought beginning after that year (Sebbar et al., 2011; Hanchane, 2013; (Yassine, 2018; Khalid & Ismail, 2021; Knippertz, 2004; Driouech et al., 2009).

Morocco's climate is subject to highly irregular rainfall patterns, leading to periods of drought followed by very wet spells or extreme rainfall events. The latter have become increasingly frequent in several Moroccan towns and regions, which have suffered catastrophic floods. Many historical events remain engraved forever in the collective memory of Moroccans. For example, the Ziz flood on November 5, 1965, left 25,000 inhabitants homeless and forced the construction of the Hassan Addakhil dam upstream from the town of Errachidia (1971). In addition, Morocco has been affected by cycles of drought that have accelerated since the 1980s, with negative impacts on several sectors of activity, notably water resources, agriculture, livestock farming, and forest ecosystems. These impacts have had consequences for migratory flows to neighboring towns or abroad.

Several research studies have been carried out in previous years on the spatiotemporal variability of precipitation in Morocco (Khalid & Ismail, n.d.; Salhi et al., 2019; Hanchane, 2013; Ezzine et al., 2014; Kyselý et al., 2012; Tramblay et al., 2012) Driouech et al., 2010; Martin-Vide, 2004), especially those that have used the same approach the authors intended to follow, such as the studies by (Longobardi & Villani, 2010) which analyzed the trends in annual and seasonal precipitation time series in the Mediterranean region and showed that the trends appear predominantly negative, both on an annual and seasonal scale, except for the summer period during which the trends are positive. Studies by (Kessabi et al., 2022) in the Fez-Meknes region have shown that annual rainfall is grouped into three sub-regions: the humid Atlantic zone, which receives significant amounts of rainfall in November and December; the arid Lower Moulouya zone, where the rainfall pattern is marked in spring, with maximum rainfall in April and March and a peak in autumn, concentrated in October and November; and the transition zone between the two zones, which extends over the Middle Atlas and the Rif, with maximum rainfall in November and April as well as minimum rainfall in May, January, and February. Their studies on the analysis of seasonal precipitation trends led to the conclusion that annual precipitation shows a downward trend in all seasons, with the exception of autumn, which shows a non-significant upward trend.

The main results obtained by (Addou et al., 2023) on the spatiotemporal variability of rainfall in the Moulouya watershed in eastern Morocco are as follows: the western and north-western part of the Middle Atlas range is exposed to disturbances from the north and west as well as experiences a winter regime, whereas the heart of the Moulouya watershed constitutes an arid zone and experiences a spring regime. In short, these studies have shown that the north-eastern and north-central parts of Morocco experience significant spatiotemporal variability in precipitation, marked by a decrease in annual rainfall.

The present study is spread over a large spatial area, encompassing a wide range of geographical features reflecting local climatic factors: continentality, orography, and slope exposure. The aim of this study was to analyze the spatial and temporal variability of precipitation in the Daoura watershed in order to understand the rainfall characteristics of this region and to ensure that the study area has experienced a significant upward trend in precipitation since the 1990s.

The present study attempted to answer the following hypotheses:

- the orographic factor is responsible for the spatiotemporal variability of precipitation between the upstream and downstream parts of the Daoura watershed;
- the size of the study area implies spatiotemporal variability in rainfall;
- the region studied is among those in the country that have experienced a significant upward trend in precipitation since the 1990s.

As a result, the Daoura watershed is the most vulnerable to climate change. The few sedentary communities are found in the oasis of the Daoura basin, which are sometimes mistaken for rivers. The water supplies in this delicate environment are significantly more than these environments can support, as demonstrated by the effects of climate change and human activity. Therefore, assessing regional climate projections requires an awareness of recent climate fluctuations. Numerous scholarly investigations have concentrated on these arid regions of the nation, always emphasizing the challenge of managing water resources in light of the potential consequences of climate change (Martin, 2006; Quintal-Marineau, 2010; Hsain, 1996).

DATA AND METHODS

Description of the studied site

The study area is approximately 35.000 km^2 and is bounded to the north by the Moulouya basin, to the north-west by the Oum Errabia basin, to the west by the Draa basin, to the east by the Guir basin, and to the south by Algerian territory. It corresponds to the Daoura watershed with its Ziz, Rhériss, and Maider tributaries. It includes the provinces of Zagora, Tinghir, Errachidia, and Midelt (Fig. 1). The region chosen as an example for this study is located in the extreme south-east of Morocco, between 30°30 and 32°30 north parallel and 3°30 and 6° west longitude. In addition, the Daoura watershed represents 4.92% of the Kingdom's total surface area. The Anti-Atlas and the Eastern High Atlas serve as topographic boundaries to the west and north, respectively, and they climax above 3600 meters. These mountains stand in the way of both oceanic and western atmospheric penetration.

The subtropical latitudinal position of the study area, combined with its landlocked continental location, form a unique landscape entity in the transition between the Mediterranean and the Great Sahara. The marked aridity of the basin is due to two essential factors: climatic demand, expressed by potential evapotranspiration, which, on average, exceeds the supply of rainwater throughout the year, and insufficient and extremely variable rainfall. Water resources depend entirely on the surface hydrographic network, which is fed by rain and snowfall from the Eastern High Atlas.

Data

The data obtained was provided to the hydraulic agency Guir-Ziz-Rheriss on an official request to the director of the hydrological agency. The Guir-Ziz-Rheriss Water Basin Agency has

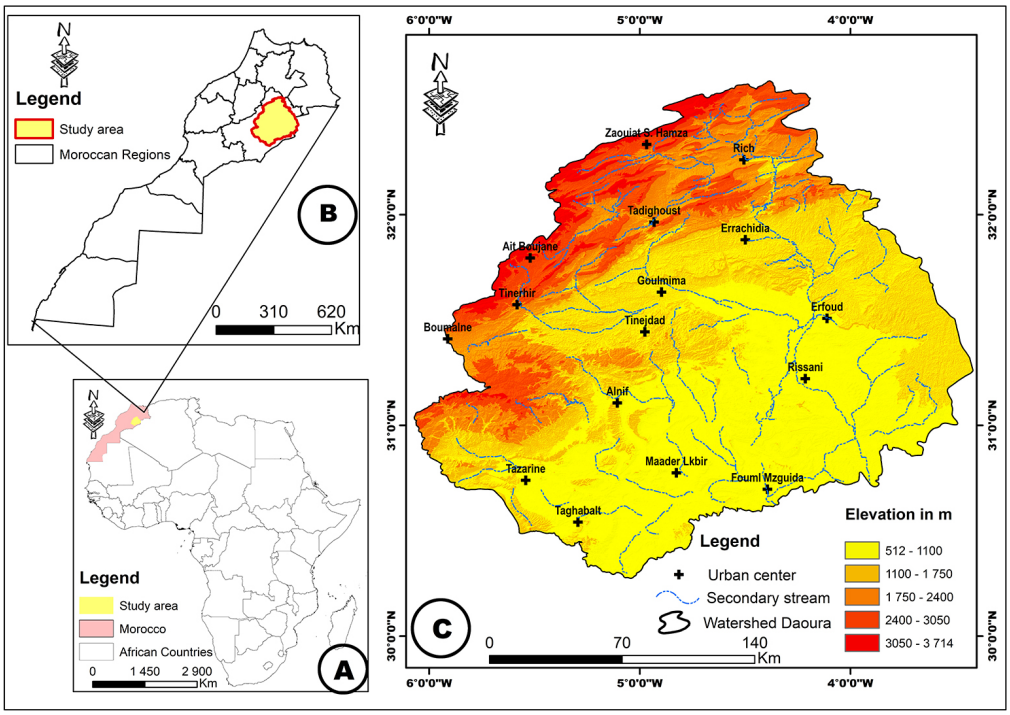

Figure 1. Study area

a network of rain stations that mainly measure rain data. The choice of resorts is an indispensable step in any climate study. Initially, the author tried to integrate as many stations as possible that are best spatially distributed across the territory of the study area and that offer a long series of observations. The monthly pluviometric data obtained concerned 13 stations with an observation period of slightly more than 61 calendar years (1957–2018) (Table 1). They cover all bioclimates in the study area, from semi-arid to Saharan. Table 1 presents other geographical statistics, such as height, duration of observation period, and percentage of missing data, whereas Figure 2 displays the spatial distribution of the measuring stations.

Methods

The Climatol tool (version 4.0.0), a computer package developed under R by Guijarro Pastor et al. (2017), and Azorin-Molina et al. (2018), is used for rainfall data homogenization. Its application

Table 1. Geographical location of rainfall stations in the study area

ID	Stations	X (°N)	Y (°W)	Z (m)	Begin year	End year	Missing data (%)
S1	Zaouiat Sidi Hamza	32.43	-4.71	1665	1970	2017	29.56
S2	FoumTillicht	32.32	-4.55	1600	1975	2018	35.44
S3	Mzizel	32.26	-4.76	1441	1970	2018	25
S4	Foum Zaabel	32.16	-4.36	1230	1970	2018	29.97
S5	Hassan Addakhil Dam	31.99	-4.48	1130	1973	2018	25.80
S6	Amouguer	31.96	-5.11	1400	1982	2017	40.99
S7	Tadighoust	31.85	-4.93	1150	1962	2018	11.15
S8	Errachidia	31.93	-4.43	1028	1965	2018	15.05
S9	Ait Boujaine	31.45	-5.56	1350	1961	2017	6.45
S10	Merroutcha	31.55	-4.89	950	1977	2018	35.21
S11	Alnif	31.13	-5.18	875	1977	2017	35.48
S12	Tazarine	30.79	-5.57	854	1995	2017	61.82
S13	Erfoud	31.53	-4.18	823	1957	2017	0

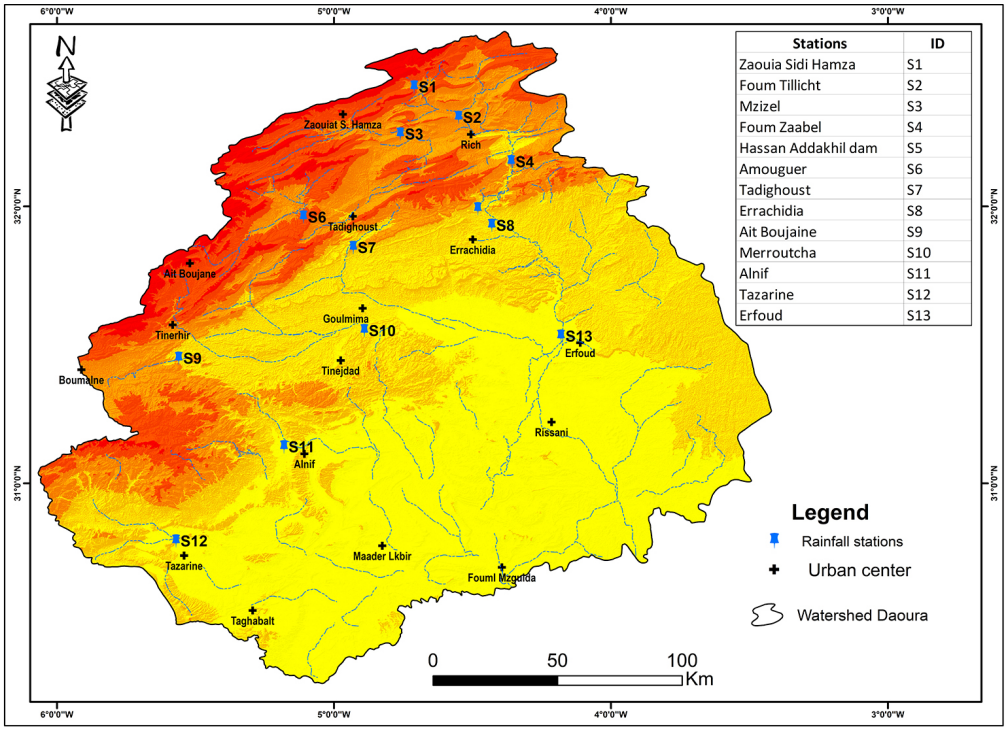

Figure 2. Geographical location of meteorological stations in the Daoura watershed

has been carried out in numerous studies and for several climate variables (Guijarro Pastor et al., 2017; Guijarro, 2018; Nimac et al., 2021; Azorin-Molina et al., 2018; Coll et al., 2020; Curci et al., 2021) compared it with other homogenization techniques they looked at, such as HOMER, ACMANT, and AHOPS, and confirmed that it could eliminate systematic mistakes associated with average jumps. It has recently been applied to the data from the Fez-Meknes region and the basins of Souss-Massa and Moulouya in Morocco.

A long series of high-quality data is needed to better understand changes in precipitation. On the other hand, measurement conditions often change. Breakpoints, also known as inhomogeneities, in climate data series that are not brought on by climatic change can be brought on by station transfers, instrument modifications, adjustments to the measurement period, environmental changes, or even adjustments to the observer making the observations. Therefore, homogenization is required to identify the true changes linked to climate change. Completing missing data is also a challenge because data sets are rarely full. Numerous methods and computer programs have been developed in recent decades to standardize meteorological elements (Venema et al., 2012). These consist of ACMANT (Domonkos, 2015); CLIMATOL (Guijarro, 2018); HOMER (Joelsson et al., 2022), the Standard Normal Homogeneity Test (SNHT) (Alexandersson, 1986; Alexandersson & Moberg, 1997). It is crucial to pay close attention to the software used during the homogenization process, as the outcome may be deceptive if inhomogeneities are eliminated from the data set, but the process also accidentally modifies the climate change signal.

The Climatol tool (version 4.0.0) (https://www.climatol.eu/accessed October 21, 2023), created by Guijarro, was utilized to solve these issues. Utilizing a modified version of the Paulhus & Kohler technique, using the nearest normalized data at each time step as the average (perhaps weighted) for all data, Climatol is an open-source R function. All that is required for normalization is scaling by the corresponding series means. After that, series anomalies are computed, outliers and series homogeneity are examined, and any missing data is filled in. This approach was selected due to its simplicity and ability to incorporate data from neighboring stations even in the absence of a similar observation period with the problematic series, which would otherwise make regression model fitting impossible (Guijarro Pastor et al., 2017). The adopted comprehensive methodology, the rainfall stations we employ, the primary procedures for verifying, reconstructing, and homogenizing rainfall anomalies in the Daoura watershed, and an analysis of the general trends in rainfall from 1957 to 2018 are all presented in this paper. Simultaneously, regionalization of the Daoura stations', which is derived from the homogenization procedure executed by the Climatol program (version 4.0.0) was showcased.

For all of the rainfall stations under investigation, the homogenization process was used in two stages in this study: the first, or exploratory stage, began after the raw data had been processed, and the second stage involved modifying SNHT1 and SNHT2 as well as the outlier acceptance threshold based on the data from the first homogenization. Better outcomes are obtained when homogeneous clusters are built using this process. The SNHT test is used to identify inhomogeneities and perform quality control of the operation using predetermined thresholds.

During the model fitting phase, a linear regression model with the formula $y = \alpha + \beta x + \varepsilon$ is assumed. The independent and dependent variables in this model are denoted by y and x, respectively, and the OLS regression coefficients are ε and β. The slope coefficient RMA is $\beta RMA = \beta/|ryx|$, where ryx is the Pearson correlation coefficient between y and x. The standard error S.E. of βRMA is equal to the S.E. f β. The RMA intercept coefficient is $\alpha RMA = y-\beta RMA$, and its standard error is equal to that of α (Zhang et al., 2005). Until the means stabilized, this approach was applied repeatedly during the homogenization process to compute and estimate missing data in the conducted series based on fitting linear relationships between nearby stations.

The Kolmogorov-Smirnov (K-S) test is a nonparametric statistical test that determines whether the underlying distribution of two candidate data sets differs significantly from one another. It is used to evaluate and examine the trend distinctions of the axis-related score time series retained by PCA (Wang, 2008). They are confirmed by cumulative distribution functions (CDFs), then the sequential Man-Kendall test (Sneyers, 1975; Mann, 1945; Sen, 1968) was used to assess the significance of the trends. Every time series was assessed as an ordered series according to the test guiding principle. Every data point in the series is contrasted with the subsequent one. The starting

value of the S statistic is set to 0, indicating that no trend has yet been identified. Then, if the observation for the next year (xj) is higher than the observation for the year before (xk), it is increased by 1, and if not, it is decreased by 1, as follows:

$$s = \sum_{k=1}^{n-1} \sum_{j=k+1}^{n} sig\,(x_j - x_k)$$
$$with: sig(x_j - x_k) = 1 \; if \; x_j - x_k > 0$$
$$sig(x_j - x_k) = 0 \; if \; x_j - x_k = 0 \quad (1)$$
$$sig(x_j - x_k) = -1 \; if \; x_j - x_k < 0$$

The final value of S is the outcome of all the increases and decreases. A trend is present when S has a strong non-zero value. However, the probability linked to S and n (sample size) is computed in order to assess the trend significance. This is done using the Z statistic, as follows:

$$Z = \frac{(S-1)}{[VAR(S)]^{1/2}} \; ; if \; S > 0 \; ; Z = 0 \; ;$$
$$if \; S = 0; Z = \frac{(S+1)}{[VAR(S)]^{1/2}}; if \; S < 0 \quad (2)$$

Z has a mean of 0 and a standard deviation of 1, suggesting that it has a normal distribution. If the probability is higher than the α% threshold (p-value), the null hypothesis is rejected. This indicates that there is less than an α% chance that the trend was discovered by accident. Therefore, at ≥ 100-α% ≒, it is statistically significant. This is a test to see if the data trend is null, or if there is no meaningful trend. The range of the p-value (α) is from 0.001 to 0.1.

RESULTS

Data verification and homogenization

Before the rainfall series under study was finally homogenized, missing data was corrected and reconstructed using the Climatol software tool. The Climatol tool defines the ratio to the mean normalization type, which allows the data from stations with noticeably varying mean rainfall to be compared (Guijarro, 2018). After examining the diagnostic diagrams of the data generated by Climatol, the threshold for accepting outliers was increased to 14 standard deviations. This was done to account for certain extreme values that fairly represent the climate of the area, particularly in mountainous areas and during particular seasons when this type of event occurs. The quality indicator file generated by the program indicates that 46.74% of the data observed as original and unmodified is present in the final database, which contains 9.672 monthly values for 13 measuring stations between 1957 and 2018 (Table 2). After comparing the data with surrounding stations, an additional 26.10% of the data were adjusted; these outliers may not accurately reflect the climate. The remaining 27.16% was made up of data that was reconstructed using the process-based method (where the contribution of neighboring stations is crucial) by Climatol software.

The essential number of data availability threshold is indicated by the red line, and the desired number by the green line. The raw data from the studied database is shown in Figure 4. The reference date was chosen as 1957 in order to have a reasonably well-covered commencement of data for the entire regional territory. The database end is determined by the need to use the most recent data accessible. There is more than enough data available to determine regional and sub-regional precipitation trends and to generate homogenized series. The essential threshold of data availability required for this package is represented by red and green lines in Figure 4, respectively. All things considered, the 1960s saw the collection of

Table 2. Main characteristics of rainfall data after the first homogenization

Data	Q. Flag	NB of data	%
Missing data	1	2627	27.16
Corrected data	2	2524	26.10
Observed data	0	4521	46.74

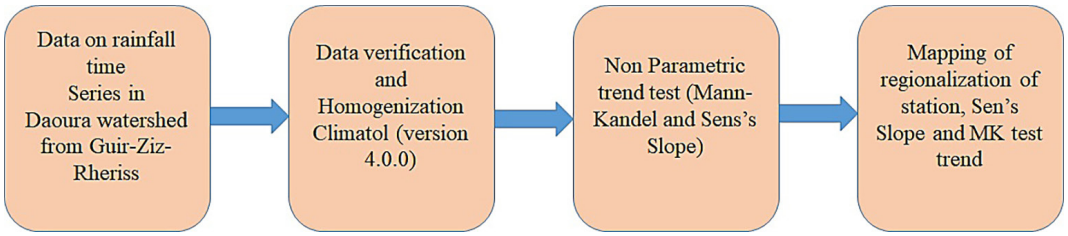

Figure 3. Methodology used in this paper

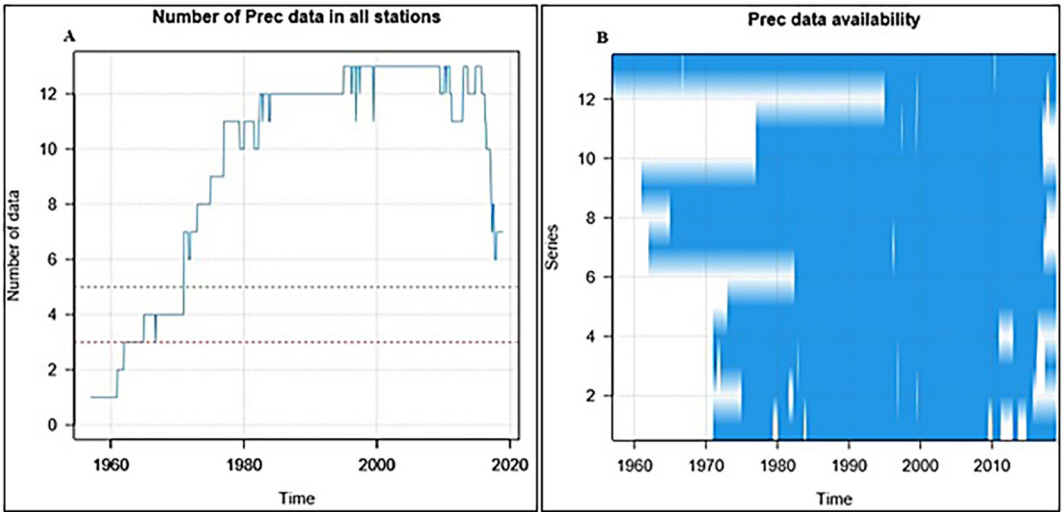

Figure 4. Data accessibility annually

more data. The network was relatively dense after 1980 until the 2010s. The degradation of the observation network had a negative impact on both the amount and quality of the data collected.

The correlograms display the correlation between the raw and homogenized data in the station series as a function of distance (calculated using first differences). A tendency favoring the homogenized data is seen in Figure 5, where the homogenization process has made up for significant, physically improbable negative correlations between a small numbers of stations. It is evident that the stations that are closer to one another-less than 50 km-have stronger correlations. In both the original and homogenized data, there is a noticeable decline in the correlation coefficient with increasing distance. This led the authors to investigate rainfall changes in the Daoura watershed using the homogenized data.

Another statistic used to assess the quality of the database homogenization is the root-mean-square error (RMSE) between the observed and estimated data (Fig. 6). This indication ranges from a minimum of 4.5 mm to a maximum of 25.9 mm, with a median of 6 mm and a mean of 7.66 mm. For the fitted data, the SNHT (on anomaly series) standard normal homogeneity test has a minimum of 26.2 and a maximum of 41.8; the mean is 32.68, and the median is 32.45. The largest values of root-mean-square error are recorded by mountain stations, according to a comparison of station RMSEs. It has already been mentioned how difficult it is to predict or interpolate precipitation in a mountainous and rough terrain.

The mapping of the absolute differences between the annual averages of the two sets of data (Fig. 7) reveals variations in a few stations (S4 Foum Zaabel and S6 Amouguer) that are adjusted

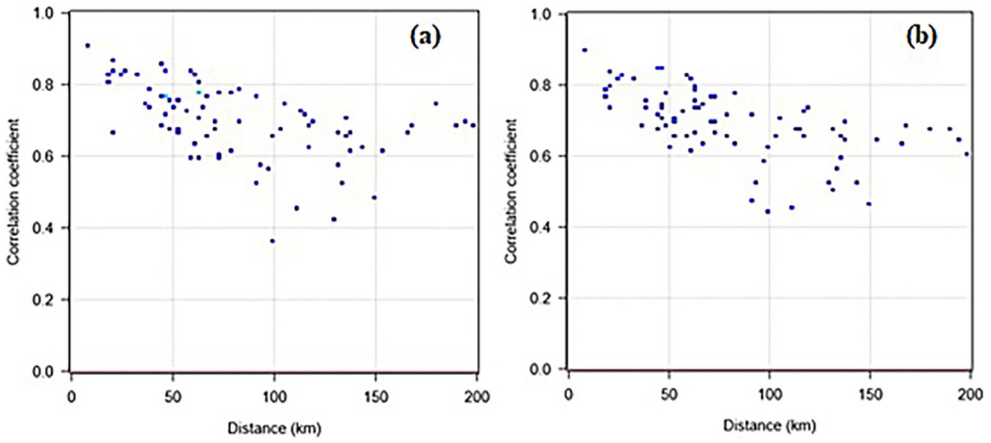

Figure 5. First difference correlograms for the series stations (a) with raw data and (b) with adjusted data

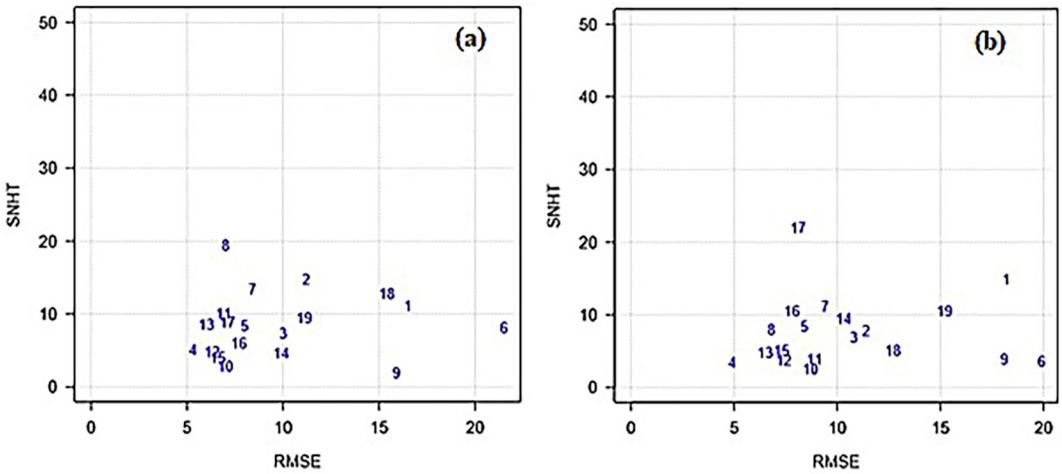

Figure 6. Plot of the raw and corrected data's quality and singularity at each station (a) and (b)

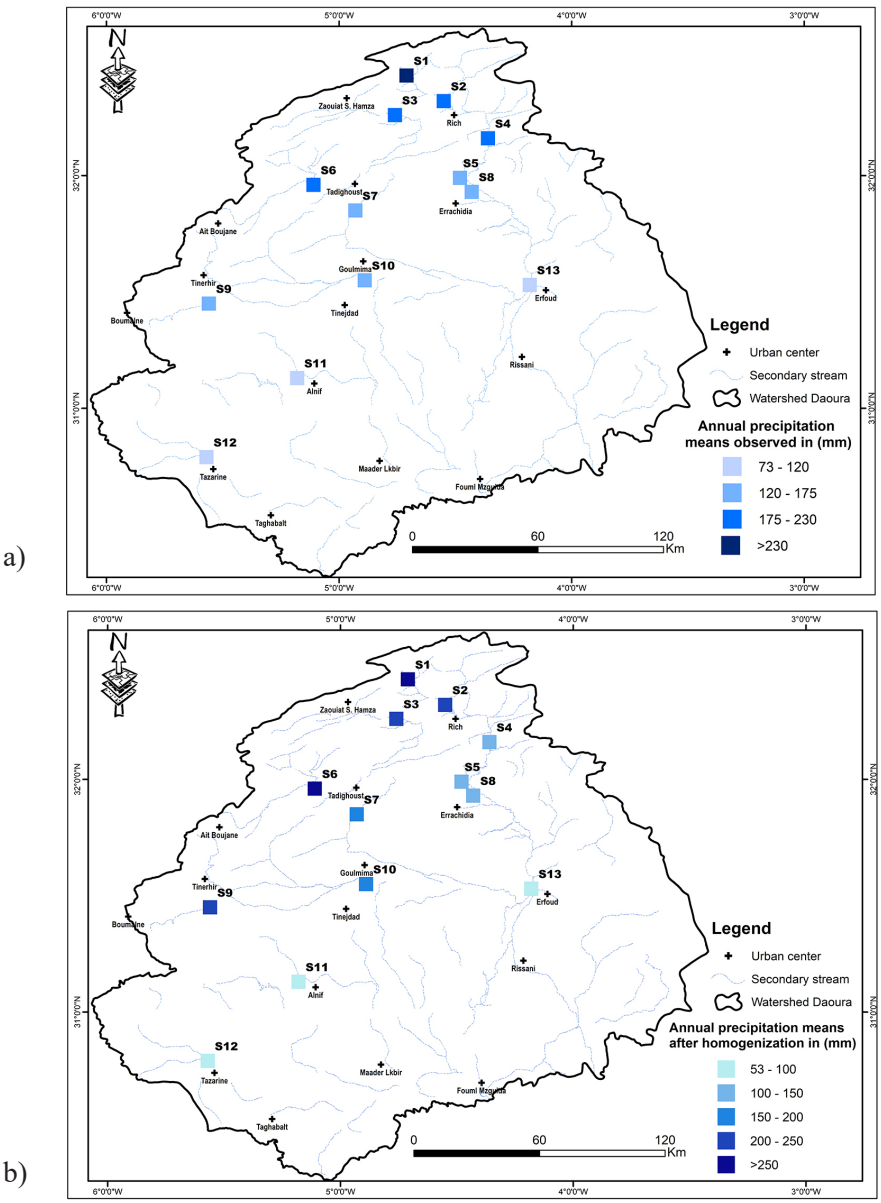

Figure 7. The absolute difference with the observed average is shown at the bottom, and a comparison of the annual averages of the two sets of data is shown at the top

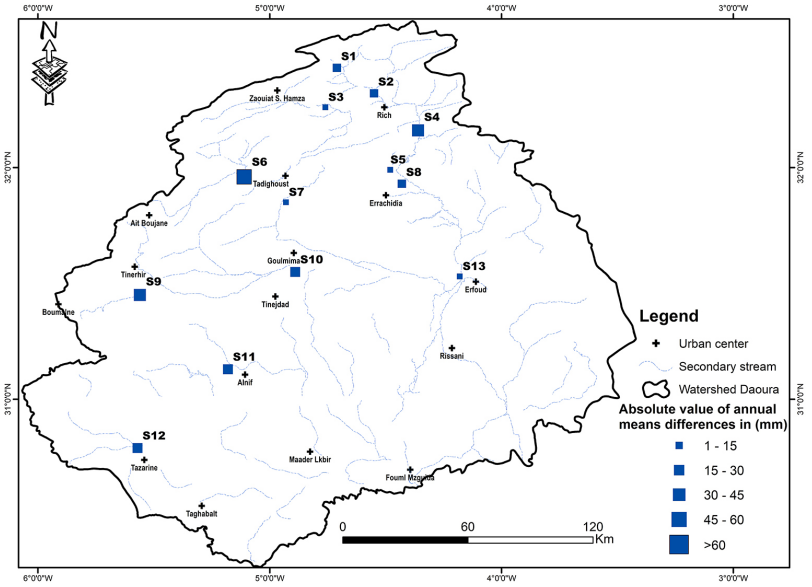

c)

Figure 7. Cont. The absolute difference with the observed average is shown at the bottom, and a comparison of the annual averages of the two sets of data is shown at the top

by homogenization techniques, since they are distant from their local climatic region. Other sites, such station S9 (Ait Boujaine), station S10 (Merroutcha), and station S12 (Tazarine), which are protected from and susceptible to the influences of the High Atlas and Anti-Atlas, were also homogenized. These stations represent a small-scale microclimate.

The comparison of the monthly averages of the raw and homogenized series shows the validity and robustness of the homogenization procedure. The temporal dispersion of the mean annual precipitation was mostly preserved despite the homogenization process. The absolute difference in mean monthly values between the two sets of data is 6.81 mm in November and 0.14 mm and 0.05 mm in May and July, respectively (Fig. 8). Height has a major impact on the spatial distribution of precipitation within the examined area because as altitude rises, the amount of precipitation varies less from upstream to downstream. For example, the Zaouat Sidi Hamza station (S1) located at the summit of the Eastern High Atlas (1665 m) receives 311 mm, but the Erfoud station located at the southernmost point of the basin receives only 72 mm. In fact, the mountain sector (of the High Atlas and Anti-Atlas) receives more rainfall than any other part of the study area. Rainfall modulus exceeds 200 mm in all High Atlas units but is less than 70 mm in the downstream part of the Daoura watershed. Rainfall is less distributed geographically increasing height and from north to south. Figure 9 illustrates the

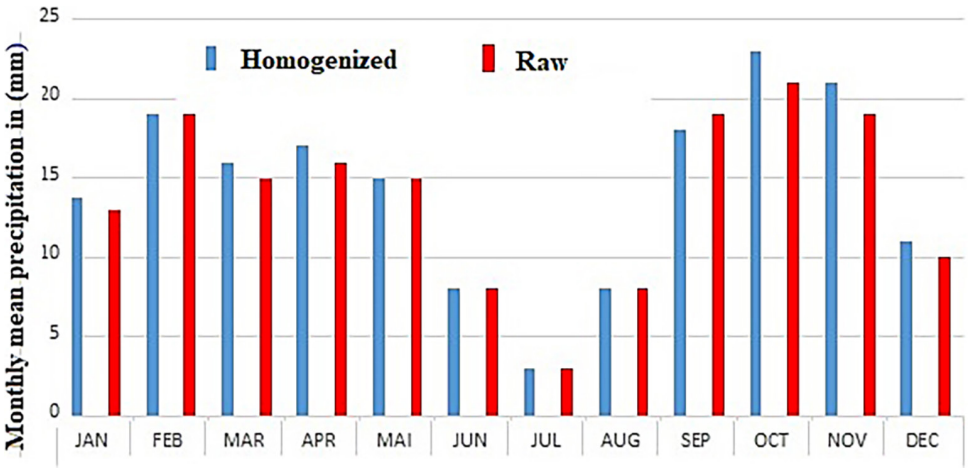

Figure 8. The region's monthly average of all available raw and normalized data

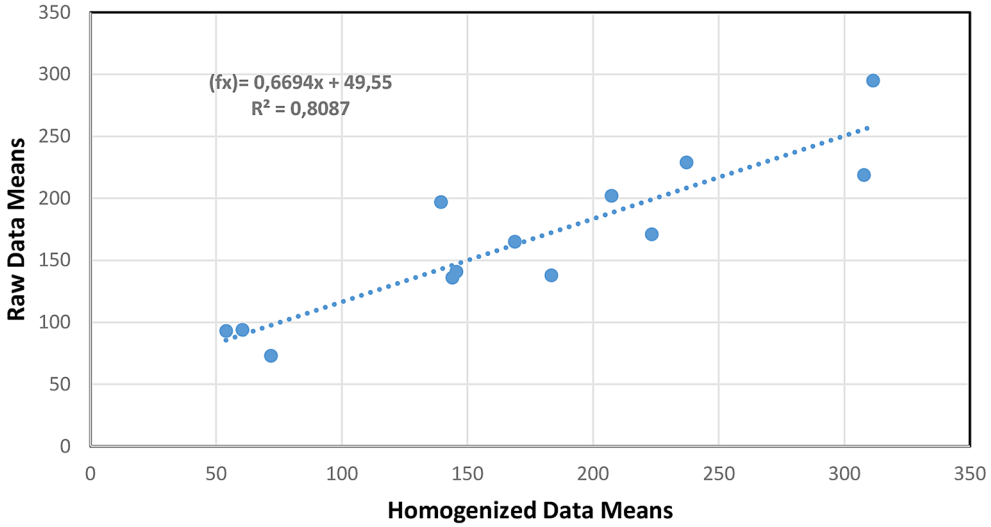

Figure 9. Correlation between the yearly means of raw and homogenized data

link between the annual averages of the homogenized data and the raw data.

A brief comparison of the results obtained from raw data and homogenized mean annual precipitation data reveals that the spatial distribution of precipitation differs from north to south. Rainfall values decrease from upstream to downstream. The downstream part of Daoura receives only ¼ of the precipitation that falls upstream. In the same sense, these values also show a spatial diversity between east and west, albeit moderate, as the average values at stations located at the same latitude (Hassan Addakhil dam-Tadighoust and Erfoud-Merroutcha) show strong differences (19 mm for the northern stations versus 49 mm for the southern stations). An analysis of average annual rainfall in the Daoura basin highlights the key role played by relief in the spatial distribution of rainfall.

Regionalization of stations

By considering the clusters or groups of stations suggested by the Climatol tool (Fig. 10), it was possible to identify three main zones, each comparatively uniform in terms of climate. Their borders are mostly determined by continental location, orography, shelter, and the direction of the prevailing winds.

The three zones are as follows: (1) a semi-arid High Atlas zone situated north of the High Atlas mountain range; (2) a transition zone (South Atlas and Anti-Atlas), situated between the peaks of the High Atlas and the Daoura sub-desert region; and (3) a sub-Saharan zone (Daoura sub-desert zone), situated south of the Daoura basin (Fig.10c).

The annual rainfall of the study area from 1957 to 2018 demonstrates significant spatial-temporal variability. Values vary from less than 60 mm at the Alnif station (S11) in the south of the study zone to 311 mm at the Zaouiat Sidi Hamza station (S1) in the north of the High Atlas Mountains and 144 mm in the Errachidia area (S8) in the center.

Semi-arid and High Atlas zone

The northern region of the study area is where this zone is situated. The rainfall trend is depicted in Figure 11, with October and November seeing the highest amounts of precipitation. The highest of 6.81 mm in October and 5.77 mm in November is the absolute difference between the monthly averages of the two types of data. For July, May, and June, the minimum values are approximately 0.05 mm, 0.14 mm, and 0.19 respectively.

The arid zone of South Atlas and Anti-Atlas

The rainfall stations located in this zone experience lower rainfall levels than the previous zone, with a large number of years below the 1957–2018 annual average (Tadighoust (S7), 36 years below average (169 mm), and Errachidia (S8), 37 years below average (144 mm). The rainfall pattern exhibits a distinct autumnal component, with October and November seeing the highest amounts, as well as January and February serving as the wintertime peak (Fig. 12). Within this zone, three sectors can be identified: the upstream Maider area near Tazarine, which has a two fold effect on the mountains

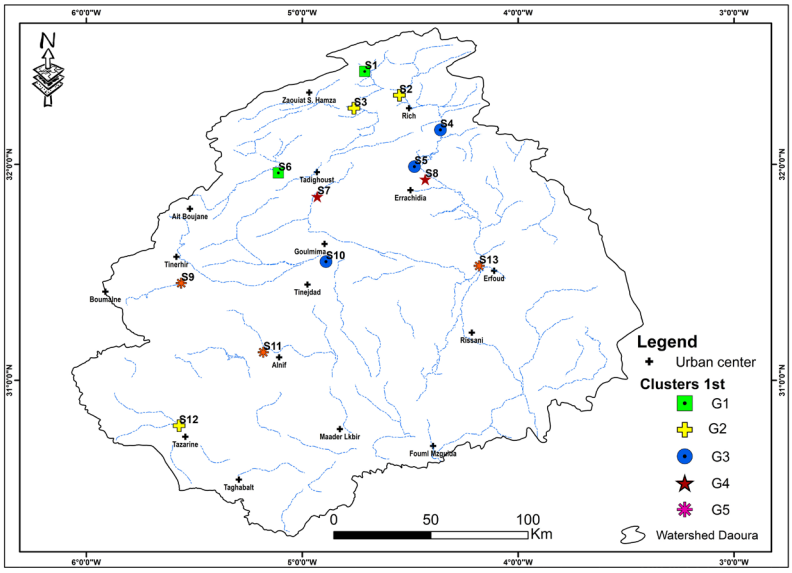

a)

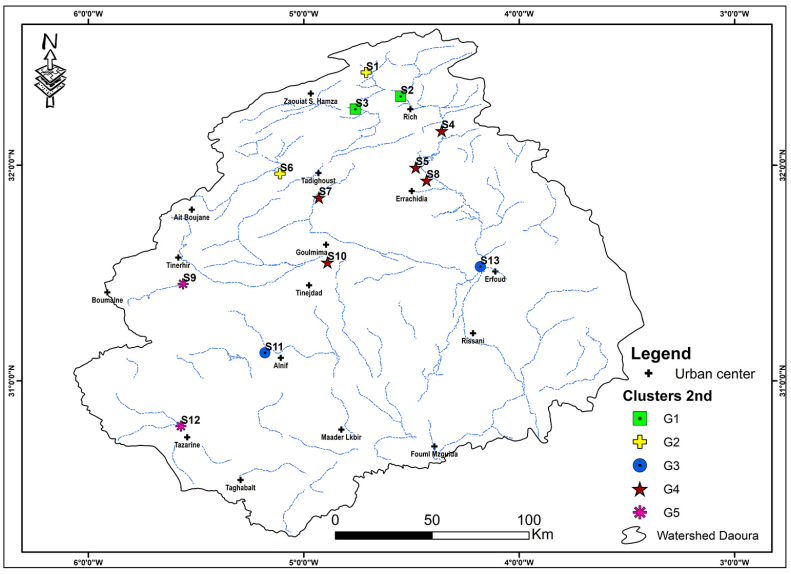

b)

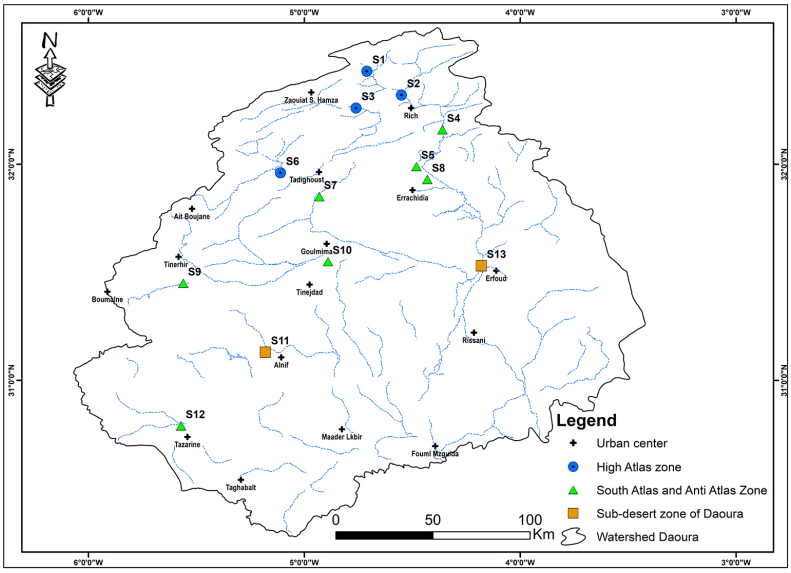

c)

Figure 10. Clusters of the rainfall stations studied (a) before and (b) after homogenization (c) generalization map

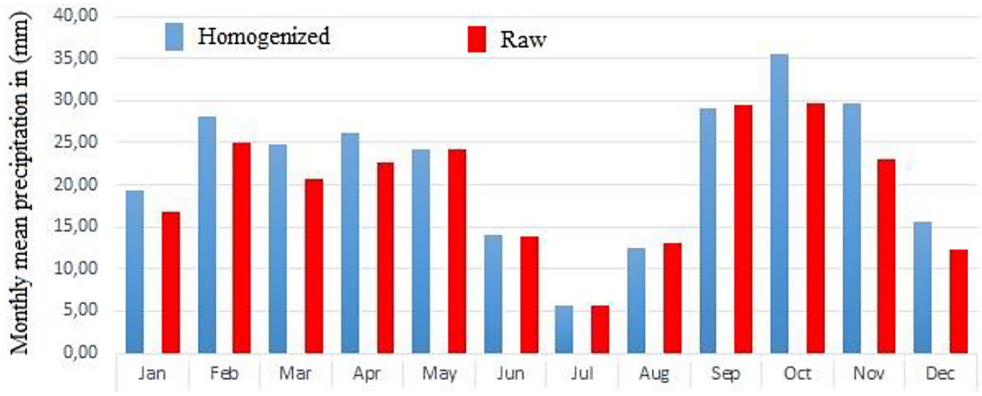

Figure 11. Monthly averages of the High Atlas and Semi-Arid zones' raw and homogenized data

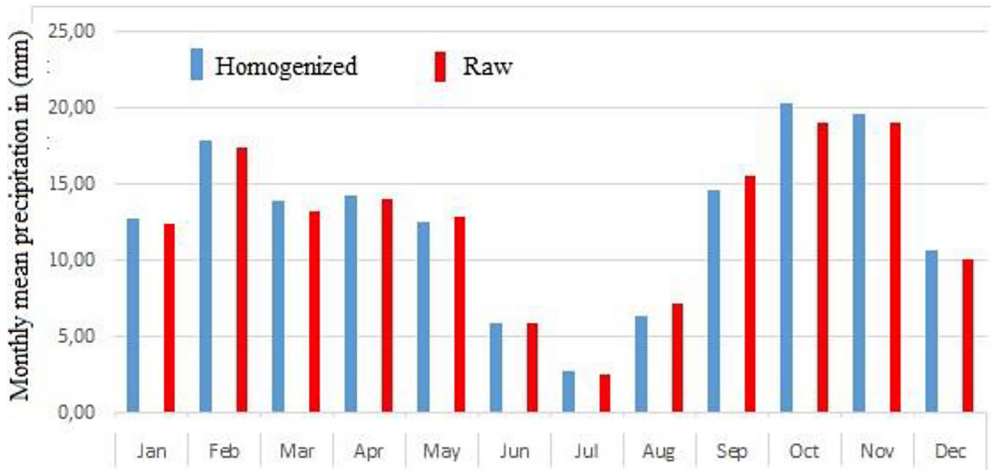

Figure 12. Monthly averages of the South Atlas and Anti-Atlas desert zone's raw and homogenized data

and the Sahara, which infiltrates through the Anti-Atlas; and the upstream Ziz and Rhériss zone (S4, S5, S7, S8, S9, and S10) with semi-arid inputs to the north.October and September have the highest absolute differences between the monthly averages of the raw and homogenized data, ranging from 1.34 mm to 0.87 mm. June has a minimum of about 0 mm, while April and July have minimums of 0.21 to 0.23 mm.

Sub-desert zone of Daoura

Between 1957 and 2018, the rainfall stations in this area had an average yearly precipitation of between 72 and 54 mm. In actuality, this time of year is usually dry. Similarly, it was found that the stations (Alnif, 38 years below average 54 mm, and Erfoud, 39 years below average 72 mm) have a significant number of average dry years. The monthly averages of the raw and homogenized data show an absolute difference of 2.5 mm and 3.12 mm between October and September, respectively, representing the autumn maximum. The minimum values for July, August, and June are roughly 0.03 mm, 0.72 mm, and 1.07 mm, respectively, as shown in Figure 13. At the majority of the stations within the research area, the annual rainfall of Daoura basin from 1957 to 2018 varies greatly. These values vary from less than 70 mm on the Tafilalet plain in the Erfoud station in the south of the research zone to 311 mm on the Haut-Atlas relief in the north (Zaouiat Sidi Hamza), 140 mm in the Errachidia area in the center. Waterfall on the upper parts of the Ziz basin actually exceeds that of the Rhériss and Maider rivers (Alnif: 95 mm, Zaouiat Sidi Hamza: 311 mm, Amouguer: 180 mm, and Zaouiat Sidi Hamza: 311 mm) over the years 1957 to 2018.

Trend analysis

On raw, homogenized time series, the Mann-Kendall and Sen's Slope estimator test is used to determine the 95% and 99% levels of occurrence,

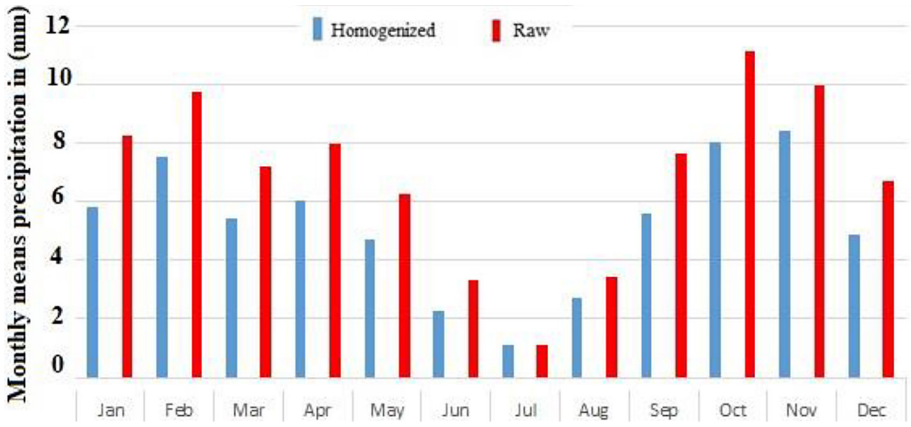

Figure 13. Monthly averages of raw and homogenized data for the sub-desert zone of Daoura

amplitude, and significance of possible annual trends (Abahous et al., 2020). Sen's slope was applied to the homogenized data and the non-parametric Mann-Kendall test was used at alpha thresholds α = 0.01, 0.05, and 0.10 to examine annual precipitation trends at all stations in the Daoura watershed. The mapped results show statistically significant negative trends at high and low altitudes (Fig.14). Thus, there is a notable variation in the quantity of trends identified. Actually, more sites with noteworthy trends are found through the homogenization process. There are noticeable wide variances in the computed trends (Rimoczi-Paal et al., 1999).

The Zaouat Sidi Hamza station (S1), which is part of the High Atlas (the upstream portion of the Daoura basin), exhibits the best distribution of highly significant positive trends. The stations situated north of the South-Atlasic furrow (S2, S3, S7, and S9), as well as the other stations in the South-Atlas and Anti-Atlas zones (S4, S5, S6, S8, S10, and S12), as well as the Daoura sub-desert zone (S11 and S13), and are not significant. Consequently, Figures 14 and 15 as well as Table 3 at the annual and monthly time scales display the most intriguing trend test results along with their statistical significance at confidence levels ranging from 90% to 99%, respectively. Monthly trends show statistically significant positive trends, particularly in the months of March, August, and September.

Prior to homogenization, data from 5 stations (S2, S3, S6, S7, and S8) exhibit a statistically significant negative trend (α = 0.05), whereas 3 stations (S1, S9, and S10) show a significant negative trend (α = 0.01). Only homogenized data with a statistically significant negative trend at the 95% and 99% confidence levels are investigated

Table 3. Trends in monthly and yearly precipitation for all available data

ID	January	February	March	April	May	June	July	August	September	October	November	December	Yearly
S1	-1.43	0.25	-0.01	0.75	0.28**	0.00	0.00	-0.10	1.00	2.16**	1.50	1.26	0.05**
S2	-0.35	-1.40	-0.37	-0.15	0.28	0.00	0.00	0.00	-0.20	0.15	0.71	0.25	0.63
S3	-0.59	-1.24	-0.35	0.13	0.09	0.00	0.00	0.00	-0.31	0.00	0.26	0.25	0.56
S4	-0.11	-0.78	1.00	0.59	0.53	0.00	0.00	0.00	-0.12	0.96	1.65	-0.04	0.40
S5	-0.47	-1.60	-0.42	-0.58	0.03	0.00	0.00	0.00	-0.13	0.33	0.34	0.21	0.40
S6	-0.83	-0.10	-0.42	0.54	0.37**	0.00	0.00	0.00	-0.56	0.75	0.75	-0.12	0.38
S7	-0.64	-1.78	-0.81	-0.61	0.11	0.00	0.00	0.00	-0.11	0.17	0.94	0.06	0.26
S8	-0.45	-1.80	-0.16	-0.58	0.11	0.00	0.00	0.00	-0.08	0.10	0.50	-0.56	0.48
S9	-0.33	-1.01	-0.33	-0.31	0.21	0.00	0.00	0.00	-0.18	0.30	0.00	-0.10	0.89
S10	0.69	-1.47	0.50	-0.30	0.23	0.00	0.00	0.00	0.72**	0.75	1.46	-0.34	0.60
S11	-0.16	-2.50*	-0.42	-0.60	0.23	0.00	0.00	0.00	-0.18	0.20	0.68	-0.26	0.48
S12	-0.34	-1.20	-0.19	-0.72	0.44	0.00	0.00	-0.03	-0.18	1.41	1.61	0.80	0.34
S13	0.55	-0.75	0.34	-0.29	0.25	0.00	0.00	0.00	-0.14	0.30	0.14	0.19	0.89

Note: *trends with significance at 0.1; **trends with significance at 0.05; ***trends with significance at 0.01.

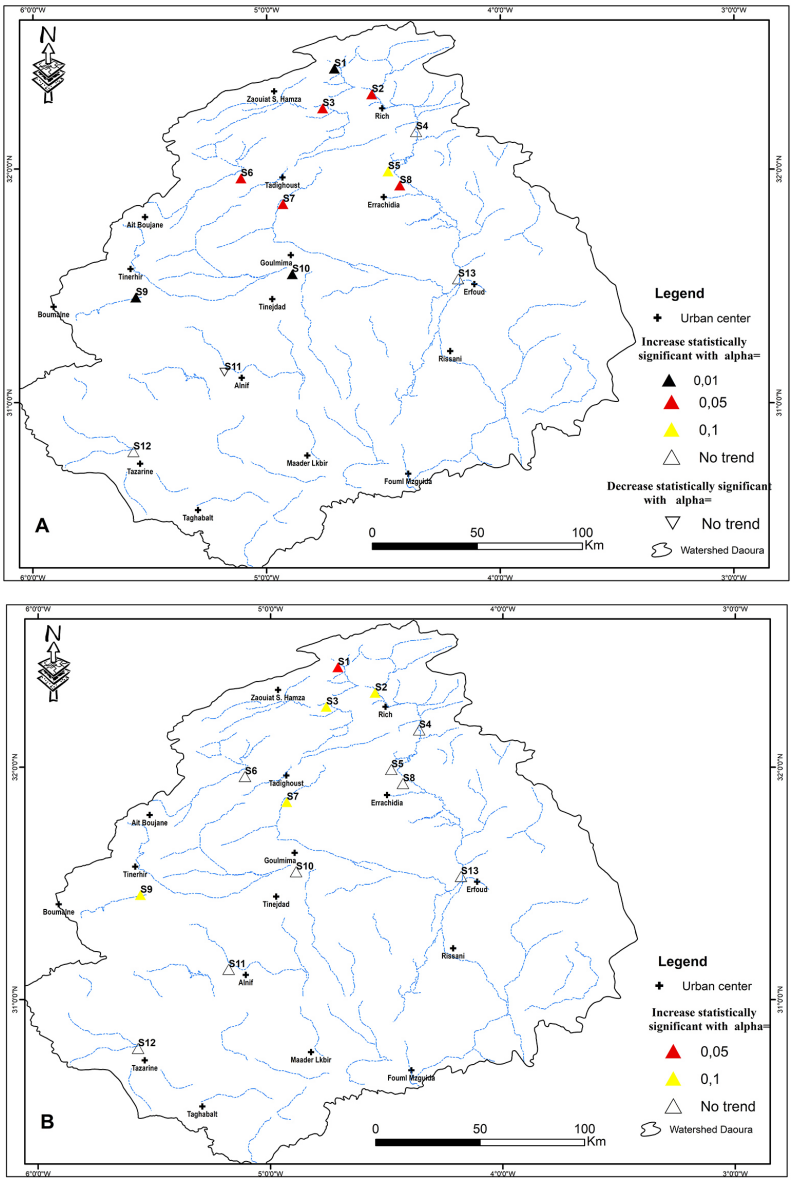

Figure 14. Significant precipitation trends' spatial distributions both before and after homogenization (a and b)

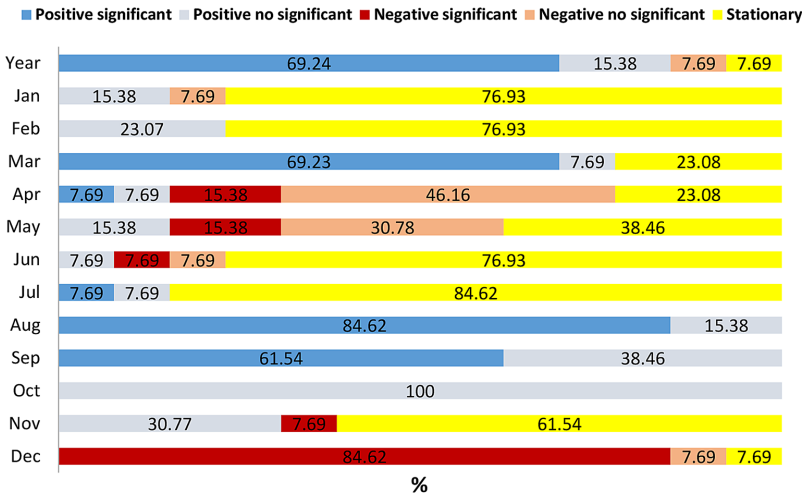

Figure 15. Percentages of grid points at the annual and monthly time periods that exhibit positive, negative, significant, non-significant, or stationary trends

in terms of country development (mm/year). At the 99% confidence level, the change values for stations exhibiting a statistically significant negative trend vary from -1.78 to -0.48. Change values vary from -2.75 to -1.05 for stations exhibiting a statistically significant negative trend at the 95% confidence level (Abahous et al., 2020).

DISCUSSION

This study first discussed the quality control and reconstitution processes for the monthly rainfall data in the Daoura watershed. Next, the study looked at the rainfall patterns in the raw and homogenized series for the years 1957–2018. The investigation of the correlograms of the raw and homogenized data indicates a high reliability of homogenization and outlier filling from a small alteration associated to data rectification and reconstitution. By figuring out the root-mean-square error that divided the raw and homogenized data for each station, the homogenization process was confirmed. A somewhat denser data network than that of Abahous et al. (2020), Kessabi et al. (2022) is revealed by an analysis of the RMSE values. Thus, the robustness and validity of the homogenization procedure are demonstrated by the fact that, except for the Amouguer station (S6), which is exposed to a small-scale microclimate, the difference between the mean annual rainfall distribution of the raw and homogenized data does not exceed 50 mm.

The algorithm is essential in the process of grouping stations with similar rainfall patterns. This regionalization, carried out using Varimax-type principal component analysis with rotation, has broken down the stations in the Daoura watershed into three distinct sub-regions with different temporal rainfall variability. The High-Atlas subregion is characterized by its autumnal regime and is more abundant in rainfall. The Arid zone of South Atlas and Anti-Atlas, which receive less rainfall and are characterized by a late, transient pattern compared with the first sub-region, and the Daoura sub-desert sub-region, which also receives less rainfall, have an autumnal rainfall pattern and stormy rainfall. On the basis of the results of this regionalization of rainfall in the Daoura, it is important to identify certain studies that have had results similar to or close to ours, such as the work of Ward et al. (1999), Singla et al. (2010), Hanchane (2013), Abahous et al. (2020), Kessabi et al. (2022), Addou et al. (2023), and Yassine (2018).

After analyzing rainfall trends, it was possible to draw the conclusion that, contrary to the impression of Morocco as a whole provided by studies like Tramblay et al. (2012), monthly rainfall has been trending much more upward in the High Atlas and south of the South-Atlasic furrow, while the sub-desert zone of the Daoura watershed has shown the opposite trend. Hence, in contrast to the downstream portion of the region, the upstream and median portions have seen a considerable rise in yearly rainfall volume due to the increase in monthly rainfall. Conversely, the annual rainfall in the High Atlas region has not been significantly affected by the rise in rainfall (1957–2018).

According to Born et al. (2008), the Daoura basin is located in the south-west Atlantic rainfall area, where yearly rainfall has been decreasing since the 1980s. The main sources of precipitation are strong showers and thunderstorms, which are most common in the fall and spring. According to Born et al. (2008), they are connected to high-altitude ridges that have their origins in the subtropics. On the other hand, winter precipitation is linked to low-pressure systems that originate southwest of the Iberian Peninsula. While the majority of climate studies carried out on Moroccan synoptic stations have shown a decrease in rainfall since the mid-1970s (Driouech et al., 2010; Driouech et al., 2021; Sebbar et al., 2011; Hanchane, 2010), especially in March (Hanchane, 2010).

The rainfall data used in this scientific paper were heterogeneous due to several conditions. To overcome the data problem, the authors proceeded to correct and fill in the anomalies to make them homogeneous and reliable using the Climatol tool (version 4.0.0), which has been used successfully in several studies (Curci et al., 2021; Guijarro, 2017; Abahous et al., 2020; Kessabi et al., 2022; Addou et al., 2023).

CONCLUSIONS

This study examined the spatial and temporal variability of rainfall in the Daoura watershed in the face of the problem of spatial and temporal discontinuity in rainfall data. On a national scale, a number of studies have been carried out on the reconstitution and homogenization of rainfall series and the study of rainfall variability and trends. The authors chose Climatol algorithms to

carry out the data reconstitution process based on the suggestions of several research studies. In the conducted study, it appears reliable and operational in terms of control, reconstitution, homogenization of rainfall data, verification of results, and grouping of rainfall stations with similar rainfall aspects. The regionalization of monthly rainfall has enabled to distinguish: (i) the High Atlas zone; (ii) the South Atlas and Anti-Atlas zone; (iii) and the Daoura sub-desert zone. The frequency analysis of monthly rainfall patterns showed that monthly peaks vary according to whether or not the climatic year is normal; in dry years, the totally dry month is July for the 3 sub-regions, whereas in extremely wet years, the rainfall maximum is recorded in October for sub-regions 1 and 2 and November for sub-region 3.

The data fitted with the Climatol homogenization procedure (version 4.0.0) has the maximum root-mean-square error of 89 mm. This error is also used to evaluate the effectiveness of the applicable methods. The most significant changes in the data attributes are indicated for trend analysis. At 95% and 99% confidence levels, homogenization makes it possible to identify more statistically significant negative trends.

Acknowledgments

We would like to thank the ABHGZR and AOEFP teams for providing data.

REFERENCES

1. Abahous H., Guijarro J.A., Sifeddine A., Chehbouni A., Ouazar D., Bouchaou L. 2020. Monthly precipitations over semi-arid basins in Northern Africa: Homogenization and trends. International Journal of Climatology, 40(14), 6095–6105.
2. Addou R., Hanchane M., Krakauer N.Y., Kessabi R., Obda K., Souab M., Achir I.E. 2023. Wavelet Analysis for Studying Rainfall Variability and Regionalizing Data: An Applied Study of the Moulouya Watershed in Morocco. Applied Sciences, 13(6), 3841.
3. Alexandersson H. 1986. A homogeneity test applied to precipitation data. Journal of Climatology, 6(6), 661–675.
4. Alexandersson H., Moberg A. 1997. Homogenization of Swedish temperature data. Part I: Homogeneity test for linear trends. International Journal of Climatology: A Journal of the Royal Meteorological Society, 17(1), 25–34.
5. Azorin-Molina C., Rehman S., Guijarro J. A., McVicar T. R., Minola L., Chen D., Vicente-Serrano S. M. 2018. Recent trends in wind speed across Saudi Arabia, 1978–2013: A break in the stilling. International Journal of Climatology, 38, e966–e984.
6. Bandhauer M., Isotta F., Lakatos M., Lussana C., Båserud L., Izsák B., Szentes O., Tveito O. E., & Frei C. 2022. Evaluation of daily precipitation analyses in E-OBS (v19. 0e) and ERA5 by comparison to regional high-resolution datasets in European regions. International Journal of Climatology, 42(2), 727–747.
7. Born C., Hardy O.J., Chevallier M., Ossari S., Attéké C., Wickings E.J., Hossaert-Mckey M. 2008. Small-scale spatial genetic structure in the Central African rainforest tree species Aucoumea klaineana: a stepwise approach to infer the impact of limited gene dispersal, population history and habitat fragmentation. Molecular Ecology, 17(8), 2041–2050.
8. Coll J., Domonkos P., Guijarro J., Curley M., Rustemeier E., Aguilar E., Walsh S., & Sweeney J. 2020. Application of homogenization methods for Ireland's monthly precipitation records: Comparison of break detection results. International Journal of Climatology, 40(14), 6169–6188.
9. Curci G., Guijarro J.A., Di Antonio L., Di Bacco M., Di Lena B., Scorzini A.R. 2021. Building a local climate reference dataset: Application to the Abruzzo region (Central Italy), 1930–2019. International Journal of Climatology, 41(8), 4414–4436.
10. De Luis M., Raventós J., González-Hidalgo J.C., Sánchez J.R., Cortina J. 2000. Spatial analysis of rainfall trends in the region of Valencia (East Spain). International Journal of Climatology: A Journal of the Royal Meteorological Society, 20(12), 1451–1469.
11. Domonkos P. 2015. Homogenization of precipitation time series with ACMANT. Theoretical and Applied Climatology, 122(1–2), 303–314.
12. Driouech F., Déqué M., Mokssit A. 2009. Numerical simulation of the probability distribution function of precipitation over Morocco. Climate Dynamics, 32, 1055–1063.
13. Driouech F., Mahé G.I.L., Déqué M., Dieulin C., El Heirech T., Milano M., Benabdelfadel H., Rouché N. 2010. Evaluation d'impacts potentiels de changements climatiques sur l'hydrologie du bassin versant de la Moulouya au Maroc. Global Change: Facing Risks and Threats to Water Resources, 561–567.
14. Driouech F., Stafi H., Khouakhi A., Moutia S., Badi W., ElRhaz K., Chehbouni A. 2021. Recent observed country-wide climate trends in Morocco. International Journal of Climatology, 41, E855–E874.
15. Emberger L. 1971. Travaux de botanique et d'écologie.
16. Ezzine H., Bouziane A., Ouazar D. 2014. Seasonal comparisons of meteorological and agricultural drought indices in Morocco using open short

time-series data. International Journal of Applied Earth Observation and Geoinformation, 26, 36–48.

17. Guijarro J.A. 2017. Daily series homogenization and gridding with Climatol v. 3. Proc. Ninth Seminar for Homogenization and Quality Control in Climatological Databases and Fourth Conf. on Spatial Interpolation Techniques in Climatology and Meteorology, 175–180.
18. Guijarro J.A. 2018. Homogenization of climatic series with Climatol. Reporte Técnico State Meteorological Agency (AEMET), Balearic Islands Office, Spain.
19. Guijarro Pastor J.A., López Díaz J.A., Aguilar E., Domonkos P., Venema V.K.C., Sigró J., Brunet M. 2017. Comparison of homogenization packages applied to monthly series of temperature and precipitation: the Multitest project.
20. Hanchane M. 2010. Impact des changements climatiques sur la tendance des précipitations annuelles, mensuelles et journalières en climats aride, semi-aride et subhumide marocains, 1961-62-1990-91.
21. Hanchane M. 2013.Méthodologie de régionalisation spatio-temporelle pour une analyse des précipitations (1961–1992): application au Maroc atlantique.
22. Hoerling M., Eischeid J., Perlwitz J., Quan X., Zhang T., Pegion P. 2012. On the increased frequency of Mediterranean drought. Journal of Climate, 25(6), 2146–2161.
23. Hsain I. 1996. Small-scale irrigation in a multiethnic oasis environment: the case of Zaouit Amelkis village, southeast Morocco. Journal of Political Ecology, 3(1), 89–106.
24. Joelsson L.M.T., Sturm C., Södling J., Engström E., Kjellström E. 2022. Automation and evaluation of the interactive homogenization tool HOMER. International Journal of Climatology, 42(5), 2861–2880.
25. Kessabi R., Hanchane M., Guijarro J.A., Krakauer N.Y., Addou R., Sadiki A., Belmahi M. 2022. Homogenization and trends analysis of monthly precipitation series in the fez-meknes region, Morocco. Climate, 10(5), 64.
26. Khalid O., Ismail E.-K. 2021. Caractéristiques et causes des sécheresses hydroclimatiques aux bassins versants méditerranéens du Rif occidental.
27. Knippertz P. 2004. A simple identification scheme for upper-level troughs and its application to winter precipitation variability in northwest Africa. Journal of Climate, 17(6), 1411–1418.
28. Kyselý J., Beguería S., Beranová R., Gaál L., López-Moreno J.I. 2012. Different patterns of climate change scenarios for short-term and multi-day precipitation extremes in the Mediterranean. Global and Planetary Change, 98, 63–72.
29. Longobardi A., Villani P. 2010. Trend analysis of annual and seasonal rainfall time series in the Mediterranean area. International Journal of Climatology, 30(10), 1538–1546.
30. Mann H.B. 1945. Nonparametric tests against trend. Econometrica: Journal of the Econometric Society, 245–259.
31. Martin-Vide J. 2004. Spatial distribution of a daily precipitation concentration index in peninsular Spain. International Journal of Climatology: A Journal of the Royal Meteorological Society, 24(8), 959–971.
32. Martin S. 2006. Influence du tourisme sur la gestion de l'eau en zone aride: Exemple de la vallée du Drâa (Maroc). Université de Lausanne.
33. Medd M.M., Assani A.A., Meddi H. 2010. Temporal variability of annual rainfall in the Macta and Tafna catchments, Northwestern Algeria. Water Resources Management, 24, 3817–3833.
34. Nimac I., Herceg-Bulić I., Cindrić Kalin K., Perčec Tadić M. 2021. Changes in extreme air temperatures in the mid-sized European city situated on southern base of a mountain (Zagreb, Croatia). Theoretical and Applied Climatology, 146(1–2), 429–441.
35. Quintal-Marineau M. 2010. Gouvernance territoriale et développement durable des communautés rurales dans la vallée du Ziz au Maroc.
36. Rimoczi-Paal A., Kerenyi J., Mika J., Randriamampianina R., Dobi I., Imecs Z., Szentimrey T. 1999. Mapping daily and monthly radiation components using Meteosat data. Advances in Space Research, 24(7), 967–970.
37. Rodriguez-Puebla C., Encinas A.H., Nieto S., Garmendia J. 1998. Spatial and temporal patterns of annual precipitation variability over the Iberian Peninsula. International Journal of Climatology: A Journal of the Royal Meteorological Society, 18(3), 299–316.
38. Salhi A., Martin-Vide J., Benhamrouche A., Benabdelouahab S., Himi M., Benabdelouahab T., Casas Ponsati A. 2019. Rainfall distribution and trends of the daily precipitation concentration index in northern Morocco: a need for an adaptive environmental policy. SN Applied Sciences, 1, 1–15.
39. Sebbar A., Badri W., Fougrach H., Hsaine M., Saloui A. 2011. Étude de la variabilité du régime pluviométrique au Maroc septentrional (1935–2004). Science et Changements Planétaires/Sécheresse, 22(3), 139–148.
40. Sen P.K. 1968. Estimates of the regression coefficient based on Kendall's tau. Journal of the American Statistical Association, 63(324), 1379–1389.
41. Servat É., Paturel J.-E., Lubès-Niel H., Kouamé B., Masson J.-M., Travaglio M., Marieu B. 1999. De différents aspects de la variabilité de la pluviométrie en Afrique de l'Ouest et Centrale non sahélienne. Revue Des Sciences de l'eau, 12(2), 363–387.
42. Singla S., Mahé G., Dieulin C., Driouech F., Milano M., El Guelai F.Z., Ardoin-Bardin S. 2010. Evolution des relations pluie-débit sur des bassins

versants du Maroc. Global Change: Facing Risks and Threats to Water Resources, 679–687.

43. Sneyers R. 1975. Sur l'analyse statistique des séries d'observations. Secrétariat de l'Organisation météorologique mondiale.
44. Taibi S., Meddi M., Souag D., Mahé G. 2013. Évolution et régionalisation des précipitations au nord de l'Algérie (1936–2009). Climate and Land Surface Changes in Hydrology, IAHS Publ, 359, 191–197.
45. Tramblay Y., Badi W., Driouech F., El Adlouni S., Neppel L., Servat E. 2012. Climate change impacts on extreme precipitation in Morocco. Global and Planetary Change, 82, 104–114.
46. Venema V.K.C., Mestre O., Aguilar E., Auer I., Guijarro J.A., Domonkos P., Vertacnik G., Szentimrey T., Stepanek P., Zahradnicek P. 2012. Benchmarking homogenization algorithms for monthly data. Climate of the Past, 8(1), 89–115.
47. Wang X.L. 2008. Penalized maximal F test for detecting undocumented mean shift without trend change. Journal of Atmospheric and Oceanic Technology, 25(3), 368–384.
48. Ward M.N., Lamb P.J., Portis D.H., El Hamly M., Sebbari R. 1999. Climate variability in northern Africa: Understanding droughts in the Sahel and the Maghreb. Beyond El Nino: Decadal and Interdecadal Climate Variability, 119–140.
49. Xoplaki E., González-Rouco J.F., Luterbacher J., Wanner H. 2004. Wet season Mediterranean precipitation variability: influence of large-scale dynamics and trends. Climate Dynamics, 23, 63–78.
50. Yassine C. 2018. Hydrologie des milieux arides et présahariens du Sud-est marocain Cas du bassin versant de l'oued Daoura.
51. Zamrane Z., Mahé G., Laftouhi N.-E. 2021. Wavelet analysis of rainfall and runoff multidecadal time series on large river basins in Western North Africa. Water, 13(22), 3243.
52. Zhang L., Bi, H., Gove J.H., Heath L.S. 2005. A comparison of alternative methods for estimating the self-thinning boundary line. Canadian Journal of Forest Research, 35(6), 1507–1514.